Macromolecules

pubs.acs.org/Macromolecules

Article

Micellization of Sequence-Controlled Polyurethane Ionomers in Mixed Aqueous Solvents

Elizabeth M. Timmers, P. Michel Fransen, Jose Rodrigo Magana, Henk M. Janssen, and Ilja K. Voets*

Cite This: *Macromolecules* 2021, 54, 2376–2382

Read Online

ACCESS | Metrics & More | Article Recommendations | Supporting Information

ABSTRACT: While the impact of compositional parameters such as block length and ionic content on the micellization of (polymeric) amphiphiles is widely investigated, the influence of monomer sequence has received far less attention until recently. Here, we report the synthesis of two sequence-controlled polyurethane ionomers (PUIs) prepared via a stepwise coupling-deprotection strategy, and compare their solution association in aqueous−organic mixtures. The two PUIs are highly similar in mass and overall composition, yet differ markedly in the sequence of building blocks. **PUI-A2** comprises a polytetrahydrofuran (pTHF) block connected to an alternation of isophorone diamine (IPDA) and dimethylolpropionic acid (DMPA) units that together are also arranged in a blockwise manner. The result is a macromolecular structure with a comparatively hydrophobic tail (pTHF) and a hydrophilic headgroup, which structure is reminiscent of those of traditional surfactants, albeit much larger in size. **PUI-S2** instead resembles a bolaamphiphilic architecture with a pTHF midblock connected on either end to a singly charged segment comprising DMPA and IPDA. We detect micellization below a threshold cosolvent volume fraction (φ_{solv}) of 0.4 in aqueous−organic mixtures with tetrahydrofuran (THF), ethanol, and isopropyl alcohol. We use scattering tools to compare the aggregation number (N_{agg}) and hydrodynamic radius (R_h) of **PUI-S2** and **PUI-A2** micelles. Irrespective of the solvent composition, we observe in the micellar window of $\varphi_{solv} < 0.4$, lower N_{agg} for **PUI-S2** micelles compared to **PUI-A2**, which we attribute to packing restraints associated with its bolaamphiphilic architecture. The increase in micellar size with increasing φ_{solv} is much more pronounced for **PUI-S2** than for **PUI-A2**. The micellar mass decreases with increasing φ_{solv} for both PUIs; the effect is modest for **PUI-S2** compared to **PUI-A2** and is not observed in the most apolar cosolvent studied (THF). Upon the approach of the micellization boundary $\varphi_{solv} \approx 0.4$, both types of PUI micelles become less compact in structure, as (in most cases) PUIs are released and as micellar dimensions increase.

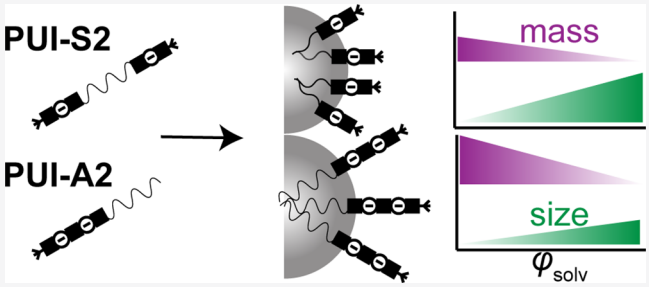

INTRODUCTION

Polyurethane ionomers (PUIs) are an interesting class of polymeric amphiphiles bearing hydrophilic, hydrophobic, and chargeable monomers.[1] They are prominently used as waterborne binders in the coating industry and also as innovative biocompatible or shape-memory materials in, for example, medical applications.[1,2] The properties and performance of PUI materials, including their behavior in aqueous media, are dependent on the complex interplay between applied synthetic procedures, solubilization techniques, emulsification and chain extension protocols, and many other factors that take place more or less concomitantly during industrial manufacturing and processing. Note particularly that PUI dispersions always contain a mixture of many different types of PUIs, varying in sequence structure, overall composition, and molecular weight. This chemical complexity affects the aqueous aggregation behavior of the PUI dispersions and, consequently, the bulk properties of the final material. For example, previous studies by others on the self-assembly of nonionic block copolymers A_nB_m and $A_{n/2}B_mA_{n/2}$ (wherein B represents the solvophobic block) revealed that, in general, AB diblock copolymers form aggregates with higher aggregation numbers and exhibit lower critical micellar concentrations (cmcs) than their ABA analogues.[3−7] The chemical complexity of waterborne PUI dispersions also obscures how chemical and physical factors, such as the aforementioned differences in the monomer sequence, determine the behavior and properties of intermediate and final products. Consequentially, the composition and production protocols of PUIs are traditionally tuned by empirical design, which has led to significant progress but does not always lead to a better understanding of, for example, unpredicted or irreproducible results. An attractive strategy to engineer new waterborne PUIs with optimal properties is to

Received: September 11, 2020
Revised: December 28, 2020
Published: February 25, 2021

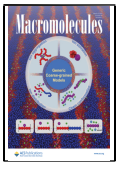

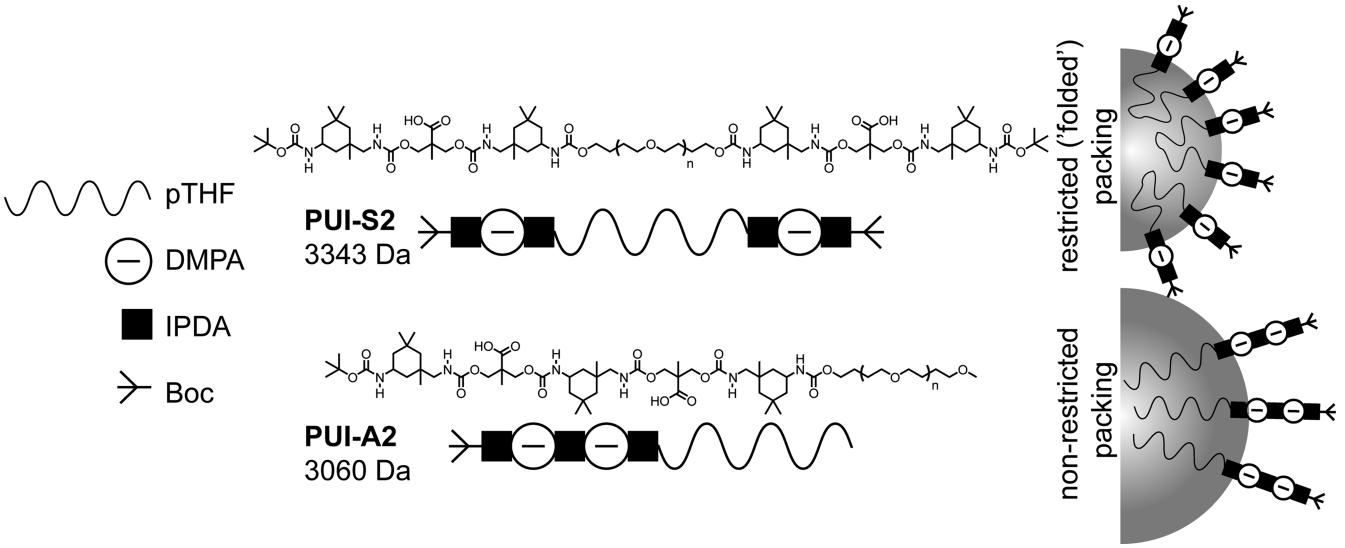

Figure 1. Left. Molecular structures and schematic representation of symmetric PUI (**PUI-S2**) and asymmetric PUI (**PUI-A2**) composed of pTHF, DMPA, IPDA, and *tert*-butyloxycarbonyl. The applied pTHF polymers have a distribution in length and molecular weight; the shown molecular weights are for $n = 27$ species (pTHF is then about 2 kDa). Right. Artist impression of packing of PUIs into spherical micelles to accommodate the ionic groups in the corona; **PUI-S2** restricted ("folded") and **PUI-A2** nonrestricted.

synthesize and study high-precision PUI polymers. Understanding the influence of the sequence and molecular architecture of PUIs on their self-assembly behavior may in future allow the smart design of novel and improved waterborne PUIs.

The synthesis of precision polymers, also known as sequence-controlled polymers, is a topic that has received great attention recently. Many different strategies aim to achieve both the highest degree of sequence regulation as well as scalability and the desired chain lengths.[8,9] Adapted from solid-phase peptide synthesis, the early examples of truly sequence-defined polymers were created from non-natural monomers (e.g., polyamides, oligocarbamates, oligosaccharides, and polypeptoids), although efforts were limited to short chain length products.[1] In contrast, controlled radical polymerizations achieve high molecular weights easily but are focused on improving the sequence regulation.[9−12] For example, Gody and co-workers produced a truly sequence-defined 15 kDa polymer in unprecedented quantities.[13] Additionally, Ouahabi and co-workers achieved a sequence-defined binary-coded polymer of nearly 17 kDa for data storage applications.[14] The solution association of precision polymers is a largely unchartered territory. The exact position of charged monomers along a chain has been shown to affect micellar aggregation number for polypeptoids[15] and to drastically affect coacervation of polypeptides because of counterion confinement.[16] Additionally, studies on poly(2-oxazoline) micelles, albeit with lower sequence regulation, found the core density to be uniform for a block sequence while nonuniform for its gradient counterpart.[17] The response to cosolvent volume fraction was more pronounced for the gradient sequence.[18]

Here, we synthesize and study the solution association of two precision PUIs, **PUI-S2** and **PUI-A2**, which are highly similar in molecular weight and composition, yet differ markedly in the sequence of molecular units. **PUI-S2** and **PUI-A2** are both prepared from polytetrahydrofuran (pTHF) with a molecular weight of about 2 kDa (pTHF2000), isophorone diamine (IPDA), and dimethylolpropionic acid (DMPA). The sequences are designed to contain the three building blocks that are frequently used in industrial mixtures at a monomer ratio of (about) 4:2:1 IPDA/DMPA/polyol as this ratio has been identified in a self-consistent field theory study as being well-suited for efficient micelle formation.[19] The structure of the asymmetric **PUI-A2** resembles the sequence of a traditional ionic surfactant with a charged headgroup and a hydrophobic tail since both DMPA monomers are located on the same chain end (**PUI-A2**, Figure 1). By contrast, the symmetric **PUI-S2** resembles a bolaamphiphilic structure, carrying one charge per chain end (**PUI-S2**, Figure 1). As the solubility of these PUIs is low, it is pertinent to study their assembly in aqueous−organic mixtures with ethanol (EtOH), isopropyl alcohol (IPA), or tetrahydrofuran (THF) as the cosolvent. We have first determined a threshold cosolvent volume fraction for association. Next, light scattering experiments have been performed to determine the dimensions and aggregation numbers of the self-assembled core−shell architectures. Based on the scaling theories developed for AB and ABA block copolymer self-assembly,[4,20] we anticipate that the PUI architecture will affect the micellar properties because of packing into more restricted ("folded") and less restricted conformations for the symmetric **PUI-S2** and the asymmetric **PUI-A2**, respectively (Figure 1).[21−23] The chain length of the PUIs is intermediate between the (macro)molecules that display this packing difference, namely, small surfactants[21,23] and large amphiphilic polymers.[22] Additionally, we expect the micellar properties to depend on the solvent composition, which affects the electrostatic repulsion between the charged DMPA monomers, the solvency of the PUIs, the preferential solvation of the various segments of the PUIs, and the solvent content of the micelle.[23,24]

EXPERIMENTAL SECTION

Materials. All reagents, chemicals, materials, and solvents were obtained from commercial sources and were used as received: Cambridge Isotope Laboratories for (deuterated) solvents; Aldrich, Acros, ABCR, Merck, and Fluka for chemicals, materials, and

https://dx.doi.org/10.1021/acs.macromol.0c02107
Macromolecules 2021, 54, 2376−2382

reagents. All solvents were of AR quality. Moisture- or oxygen-sensitive reactions were performed under an atmosphere of dry argon.

PUI-S2 and PUI-A2. The synthesis and molecular characterization of the PUI macromolecules are described in detail in the electronic Supporting Information.

Sample Preparation. PUI samples were prepared using a solvent switch strategy. To this end, the PUIs were molecularly dissolved by sonication for 10 min in EtOH, IPA, or THF containing triethylamine (TEA) in a 2:1 molar ratio of TEA/DMPA groups to ensure full ionization of the carboxylic acids due to excess of the TEA base. Next, an appropriate amount of water was added to yield aqueous−organic samples with an organic solvent volume fraction $0.1 \leq \varphi_{solv} \leq 0.9$, and these samples were sonicated for 10 min. All samples contained 1 mM PUI. Prior to light scattering measurements, the samples were filtered over an MDI PVDF (for $0.1 \leq \varphi_{solv} \leq 0.3$) or a VWR International PTFE (for $0.4 \leq \varphi_{solv} \leq 0.9$) filter with 100 nm pores. The dielectric constants, ε_{solv}, of the solvents for EtOH, IPA, THF, and H_2O at room temperature are 25, 18, 7.5, and 79, respectively.

Refractometry. The refractive index (n) of each solvent composition (in the absence of PUI) was determined using a temperature-controlled ABBE 60/ED refractometer from Bellingham & Stanley Ltd. equipped with a mercury lamp. n-values computed with the Abbe Utility Program are given in Table S2.

Viscosimetry. The dynamic viscosities (η) for each solvent composition were determined (Figure S4) using a calibrated Anton Paar Lovis 2000 ME rolling ball viscometer, measured in a 1.59 mm diameter glass capillary equipped with a gold ball (1.5 mm diameter) at room temperature and atmospheric pressure.

Static Light Scattering and Dynamic Light Scattering. Static light scattering (SLS) and dynamic light scattering (DLS) measurements were performed on an ALV Compact Goniometer System (CGS-3) instrument equipped with an ALV-7004 Digital Multiple Tau Real-Time correlator and a 40 mW solid-state laser operating at a wavelength $\lambda = 532$ nm. As the samples are dilute, we assume little to no concentration dependence and perform all experiments at a fixed concentration. The total mean scattered intensity (I_{90}) and the second-order correlation function, $g_2(t)$, were recorded at a fixed scattering angle $\theta = 90°$ in five runs of 60 s for each sample in duplicate.

AfterALV software (Dullware Inc.) based on the CONTIN algorithm was used to determine the frequency Γ from the mean $g_2(t)$, from which we compute the apparent translational diffusion coefficient, D^{app}, according to

$$D^{app} = \Gamma/q^2 \tag{1}$$

with q defined as

$$q = \frac{4 \times \pi \times n_s \times \sin(\theta/2)}{\lambda} \tag{2}$$

Note that the scattering vector q varies approximately 3% with sample composition for a fixed scattering angle of 90° because of the variations in the solvent refractive index n_s with the solvent composition ($0.0223\ nm^{-1} \leq q \leq 0.0230\ nm^{-1}$ for $0.1 \leq \varphi_{solv} \leq 0.5$ for EtOH, IPA, and THF). Using the Stokes−Einstein equation, we determine from D_{app} the apparent hydrodynamic radius, which we denote as R_h throughout this manuscript

$$R_h = \frac{k_B \times T}{6 \times \pi \times \eta \times D_{app}} \tag{3}$$

where k_B, T, and η are the Boltzmann constant, temperature, and viscosity respectively.

The Rayleigh ratio, R, is calculated from the measured scattering intensity by

$$R = \frac{(I_s - I_{bkg}) \times {n_s}^2}{(I_t - I_{dc}) \times {n_t}^2} \times R_t \tag{4}$$

where I_s, I_t, I_{bkg}, and I_{dc} are the scattering intensities of the sample, toluene reference, solvent, and dark current, respectively; n_s and n_t are the refractive indices of the sample and toluene; and R_t is the Rayleigh ratio of toluene ($R_t = 2.07 \times 10^{-5}\ cm^{-1}$).[25] I_{bkg} and I_{dc} are assumed negligibly small in comparison to I_s and I_t.

Since the PUI solutions are dilute and the micelles are small (*vide infra*), $P(q)$ and $S(q)$ are assumed to deviate little from unity. This is confirmed by SLS experiments on selected samples performed at scattering angles $50° \leq \theta \leq 150°$ (Fig. S6). The micellar mass can then be obtained from the measured excess Rayleigh ratio R according to the following simplified expression

$$R = K \times c \times M_{micelle} \tag{5}$$

where K, c, and $M_{micelle}$ are the optical constant, the PUI weight concentration, and the apparent micellar weight, respectively. K is given by

$$K = \frac{4 \times \pi^2 \times n^2 \times \left(\frac{dn}{dc}\right)^2}{N_A \times \lambda^4} \tag{6}$$

where N_A is Avogadro's number and dn/dc is the refractive index increment ($dn/dc = 0.135\ cm^3/g$).[26] The aggregation number (N_{agg}) is obtained from $N_{agg} = M_{micelle}/M_{PUI}$ (with $M_{PUI\text{-}S2} = 3343$ g/mol, $M_{PUI\text{-}A2} = 3060$ g/mol). The micellar density $\rho_{micelle}$ is obtained in a straightforward manner from the micellar mass and hydrodynamic radius according to

$$\rho_{micelle} = \frac{M_{micelle}}{N_A \times \frac{4}{3} \times \pi \times {R_h}^3} \tag{7}$$

RESULTS AND DISCUSSION

Synthesis of Sequence-Controlled PUIs. To unravel the influence of the PUI sequence on the structure of PUI micelles, we first needed to develop a reliable synthetic strategy to obtain sequence-controlled PUIs in high yield. Obtaining such macromolecules with conventional synthetic routes is highly challenging since waterborne PUIs rely on statistical reactions between alcohols and isocyanates, instantly resulting in a range of molecular structures. Additionally, the high reactivity of isocyanates makes it difficult to isolate and store isocyanate-functional intermediates as they may react slowly with ambient humidity or traces of water during purifications. To overcome these problems, we have substituted the reaction of isocyanates with alcohols to produce urethane bonds with the reaction of amines with activated carbonates. Molecules with these functional groups are stable. The reaction between amines and activated carbonates also yields urethane linkages with the advantage that the sequences can be isolated and purified conveniently after each step. To obtain the sequence-controlled PUIs in Figure 1, we have implemented a step-wise synthetic strategy using protective group chemistry and iterative coupling-deprotection syntheses. The Supporting Information provides full details on the synthesis and characterization of **PUI-S2** and **PUI-A2** and elaborates further on the structural features of these materials. The successful synthesis and macromolecular integrity of the PUI products are confirmed by ^1H NMR (details in the Supporting Information), size exclusion chromatography (Table S1), and matrix-assisted laser desorption ionization time-of-flight mass spectrometry (Figure S3) analyses.

Threshold Cosolvent Volume Fraction for PUI Micellization in Aqueous−Organic Solvent Mixtures. Aqueous dispersions of amphiphilic block copolymers generally self-organize in water into micellar structures driven by the hydrophobic effect. Tuning the hydrophilic to hydrophobic ratio, the molecular architecture and monomer

https://dx.doi.org/10.1021/acs.macromol.0c02107
Macromolecules 2021, 54, 2376−2382

sequence of the polymer grant control over micellar properties. In traditional amphiphiles, a single hydrophilic headgroup is joined directly to a single hydrophobic tail. In contrast, bolaamphiphiles have two hydrophilic headgroups connected by a hydrophobic segment. Although the chemical composition may be the same, differences in the packing parameter lead to changes in the micellar dimensions, morphology, and aggregation number.[21−23] To unravel the differences in micellization behavior of two PUIs with identical building blocks but differing sequences, the amphiphilic **PUI-A2** and the bolaamphiphilic **PUI-S2**, we first optimized sample preparation, examined the dissolution behavior, and established the solution conditions amenable to micellization.

Both PUIs, with added TEA base, associated with pure water above a threshold polymer concentration. DLS experiments revealed broad, multimodal size distributions, showing an abundance of micellar particles but also revealing large aggregates with ill-defined dimensions much larger than the length of a fully extended PUI chain (∼20 nm). These results precluded in-depth SLS studies. To circumvent these complications, we decided instead to study micellization in aqueous−organic mixtures with a sufficiently high amount of EtOH, IPA, or THF to promote PUI solvency and prepare samples in a reproducible manner, yet with a sufficiently low cosolvent content to allow for micellization.[27,28] A solvent switch strategy was applied to prepare the PUI solutions in aqueous−organic mixtures with a water volume fraction in the range $0.1 \leq \varphi_{water} \leq 0.9$ (see the Materials section for further information). To establish the solvent compositional window for micellization, we recorded the scattered intensity at 90°, I_{90}, of 1 mM **PUI-S2** and **PUI-A2** solutions as a function of the cosolvent volume fraction, φ_{solv} (Figure 2). As anticipated,

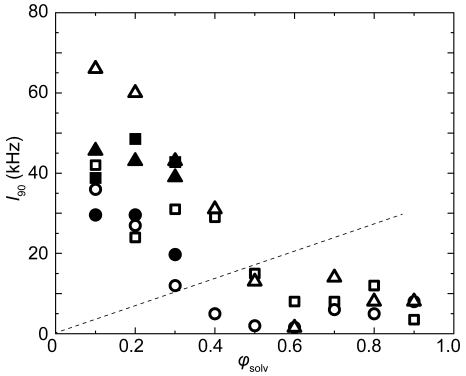

Figure 2. Scattering intensity of **PUI-S2** (solid symbols) and **PUI-A2** (open symbols) at 90° (I_{90}) as a function of φ_{solv} for aqueous−organic solvent mixtures with EtOH (triangles), IPA (circles), and THF (squares). The dashed line represents a guide to the eye indicative for the approximate micellization boundary.

both **PUI-S2** and **PUI-A2** were molecularly dissolved at high cosolvent volume fractions, as inferred by the weak scattering intensity close to the background level. An increased scattering intensity at high water and low cosolvent content ($\varphi_{solv} < 0.4$) indicated solution association below this threshold φ_{solv}. Complementary DLS experiments revealed that the samples could be prepared in a reproducible manner in this association window for φ_{solv} = 0.1, 0.2, and 0.3 for all three cosolvents. Monomodal size distributions were consistently observed, with mean values for the hydrodynamic radii well within the micellar range (i.e., far below the fully extended PUI chain length, Figure S5). The three solvent compositions φ_{solv} = 0.1, 0.2, and 0.3 were thus selected for further analysis to examine the impact of PUI sequence on the micellar structure.

Impact of Sequence and Solvent Composition on the Size and Aggregation Number of PUI Micelles. DLS and SLS experiments were performed on 1 mM **PUI-S2** and **PUI-A2** solutions in aqueous−organic mixtures with 10−30 vol % EtOH, IPA, and THF to determine the impact of PUI sequence on the size and aggregation number of PUI micelles (Figure 3, Table 1). These structural features are primarily

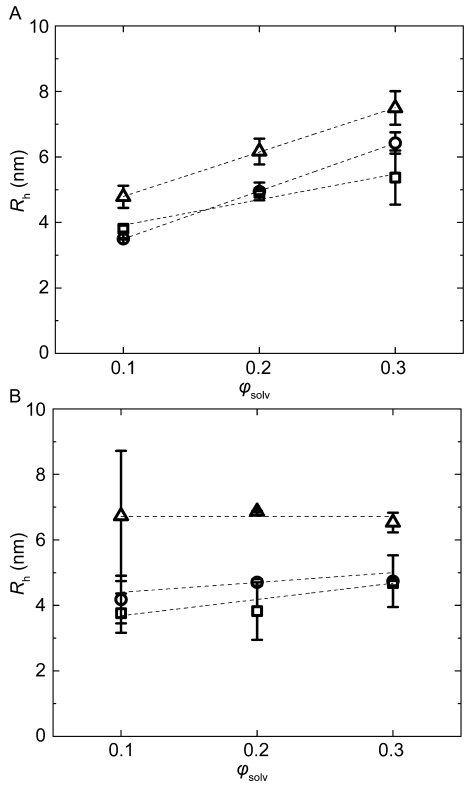

Figure 3. Mean hydrodynamic radius, R_h, for **PUI-S2** (A) and **PUI-A2** (B) as a function of EtOH (triangle), IPA (circle), and THF (square) volume fraction φ_{solv}, in water, including standard deviation.

governed by three contributions to the free energy per PUI chain within the micelle (F_{int}, F_{core}, and F_{corona}), which depend on the core-corona surface tension (F_{int}), coral monomer interaction, chain stretching and packing (F_{core}), and headgroup repulsion and conformation (F_{corona}).[20] Both micelle size and aggregation numbers depend on solvent composition for **PUI-S2** and **PUI-A2** micelles. We observe hydrodynamic radii in the range of 3.5 nm $\leq R_h \leq$ 7.5 nm for **PUI-S2** micelles and 3.8 nm $\leq R_h \leq$ 6.9 nm for **PUI-A2** micelles (Figure 3). The dimensions of both PUI micelles tend to increase with increasing φ_{solv} apart from **PUI-A2** micelles in aqueous EtOH mixtures. The increase in R_h with increasing φ_{solv} is more pronounced for **PUI-S2** than for **PUI-A2**. As a consequence, **PUI-A2** micelles tend to be somewhat larger at low and smaller at high cosolvent volume fractions compared to **PUI-S2** micelles. The higher response of **PUI-A2** to solvent fraction can be attributed to the closer proximity to the cmc, compared to **PUI-S2**, as this boundary is generally higher for ABA triblocks.[4−7] The micellar dimensions of both PUIs appear to decrease with solvent polarity ($R_{h,EtOH} > R_{h,IPA} > R_{h,THF}$). The effect may be related to differences in the electrostatic

https://dx.doi.org/10.1021/acs.macromol.0c02107
Macromolecules 2021, 54, 2376−2382

Table 1. Overview of the Molecular Weight of Assembly $M_{micelle}$, Aggregation Number N_{agg}, Apparent Hydrodynamic Radius R_h, and Overall PUI Density in the Micelles $\rho_{micelle}$ of PUI-S2 and PUI-A2 in Water/EtOH, Water/IPA, and Water/THF Mixtures at Different Solvent Volume Fractions

	PUI-S2				PUI-A2			
	$M_{micelle}$ (kDa)	N_{agg}	R_h (nm)	$\rho_{micelle}$ (g/cm^3)	$M_{micelle}$ (kDa)	N_{agg}	R_h (nm)	$\rho_{micelle}$ (g/cm^3)
φ_{EtOH} = 0.1	179.9	54	4.8	0.65	294.2	96	6.7	0.38
φ_{EtOH} = 0.2	189.7	57	6.2	0.32	261	85	6.9	0.32
φ_{EtOH} = 0.3	156.7	47	7.5	0.15	229.1	75	6.5	0.33
φ_{IPA} = 0.1	117.1	35	3.5	1.08	195	64	4.2	1.06
φ_{IPA} = 0.2	118.6	35	4.9	0.39	166.8	55	4.7	0.63
φ_{IPA} = 0.3	79.3	24	6.4	0.12	52.5	17	4.7	0.2
φ_{THF} = 0.1	154.7	46	3.8	1.12	162.9	53	3.8	1.21
φ_{THF} = 0.2	196.6	59	4.9	0.66	148.1	48	3.8	1.05
φ_{THF} = 0.3	177	53	5.4	0.45	187.1	61	4.7	0.72

repulsion between the charged DMPA monomers,[23,24] the solvency of the PUIs, the preferential solvation of the various segments of the PUIs, and the solvent content of the micelles. For example, at full DMPA ionization, because of the presence of the TEA base, the ionic headgroup repulsion may be more pronounced, resulting in smaller micellar sizes for the solvent mixture with the lowest dielectric constant, being aqueous THF mixtures.[23,24]

A pronounced decrease in N_{agg} with increasing φ_{solv} upon approach of the threshold water content for micellization is observed for **PUI-A2** in water/IPA and water/EtOH mixtures (Table 1). We find the highest N_{agg} in the ethanolic solvent mixtures comprising the cosolvent with the highest dielectric constant, which may reduce the coronal repulsion between the tightly packed (bola)amphiphiles somewhat. The aggregation numbers for **PUI-S2** micelles are approximately half that for **PUI-A2** micelles in water with IPA and EtOH, in concomitance with studies on AB diblock and ABA triblock copolymers.[4−6,22] The lower micellar mass for the bolaamphiphilic **PUI-S2** micelles is attributable to packing constraints. These PUI chains likely adopt a "folded" conformation, which is more restricted than the **PUI-A2** conformation. Unexpectedly, the values for N_{agg} are comparable in aqueous THF mixtures.

The micelles likely become less compact due to, for example, swelling as φ_{solv} increases toward the micellization boundary (Figure 4). Interestingly, both **PUI-S2** and **PUI-A2** appear most compact in aqueous THF mixtures with the lowest polarity and least compact in aqueous EtOH mixtures with the highest polarity. **PUI-S2** micelles seem somewhat less compact than **PUI-A2** micelles. This appears related to the rather low values for N_{agg}, which decrease little with increasing φ_{solv}, while R_h increases significantly with increasing φ_{solv}.

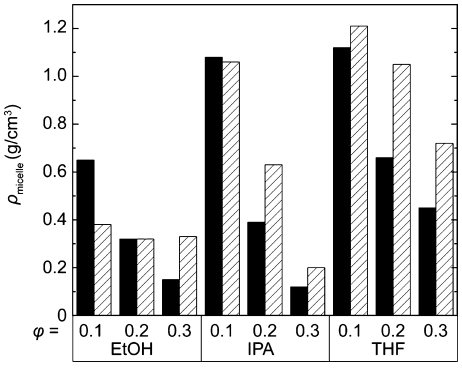

Figure 4. Micellar densities ($\rho_{micelle}$) for **PUI-S2** (solid) and **PUI-A2** (dashed) micelles as a function of the cosolvent type and volume fraction.

CONCLUSIONS

While micellization of (polymeric) amphiphiles has drawn attention for decades, the impact of the monomer sequence on the micellar structure and properties has sparsely been investigated. Here, we present and have synthesized completely novel sequence-controlled PUIs and have studied their association in solution. The sequence-controlled PUIs have nearly identical mass and composition, yet markedly different architecture: the bolaamphiphilic **PUI-S2** carries two charges on the opposite ends of the pTHF midblock, while **PUI-A2** resembles the classical head-to-tail structure as both charges are positioned on the same chain end. A stepwise coupling-deprotection synthetic protocol using activated carbonate and amine reactants was employed to produce the PUIs. Using a solvent switch approach, we prepared aqueous−organic dispersions with EtOH, IPA, or THF and determined a threshold solvent volume fraction of <0.4 for reproducible micellization to take place. In this micellar window of φ_{solv} < 0.4, **PUI-S2** micelles display slightly lower N_{agg} than **PUI-A2** micelles. We attribute this to packing restraints associated with the bolaamphiphilic architecture of **PUI-S2**. The dimensions of both PUI micelles tend to increase with increasing φ_{solv} (except for **PUI-A2** in aqueous EtOH); the swelling is most pronounced for **PUI-S2**. The micellar mass decreases with increasing φ_{solv} for both PUIs; the effect is modest for **PUI-S2** compared to **PUI-A2** and is not observed in the most apolar cosolvent studied (THF). We relate both the increase in R_h and decrease in $M_{micelle}$ with increasing φ_{solv} to a reduced driving force for micellization upon the approach of the micellization boundary $\varphi_{solv} \sim 0.4$. As φ_{solv} increases, both types of PUI micelles thus become less compact in structure as PUIs are released (**PUI-A2**) while micellar dimensions increase (**PUI-S2**). Relatively large micelles with high N_{agg} are found in water/EtOH mixtures containing the cosolvent with the highest dielectric constants, which may slightly reduce the coronal electrostatic repulsion. We hope that this work inspires further experiments on the solution association of sequence-controlled polymers as well as detailed studies on the impact of differential solvent compositions on micellar properties.

https://dx.doi.org/10.1021/acs.macromol.0c02107
Macromolecules 2021, 54, 2376−2382

■ ASSOCIATED CONTENT

Supporting Information

The Supporting Information is available free of charge at https://pubs.acs.org/doi/10.1021/acs.macromol.0c02107.

Detailed synthesis schemes, stepwise procedures, and characterization of PUIs; ^{1}H NMR spectroscopy, size-exclusion chromatography, matrix-assisted laser desorption ionization time-of-flight mass spectrometry, and high-performance liquid chromatography analyses; and data used for light scattering analysis, specifically, viscosity and refractive index measurements, size distributions from DLS and SLS on selected samples (PDF)

■ AUTHOR INFORMATION

Corresponding Author

Ilja K. Voets − *Laboratory of Self-Organizing Soft Matter, Department of Chemical Engineering and Chemistry, Eindhoven University of Technology, 5600MB Eindhoven, The Netherlands; Laboratory of Macro-Organic Chemistry, Department of Chemical Engineering and Chemistry and Institute for Complex Molecular Systems, Eindhoven University of Technology, 5600MB Eindhoven, The Netherlands;* orcid.org/0000-0003-3543-4821; Email: i.voets@tue.nl

Authors

Elizabeth M. Timmers − *Laboratory of Self-Organizing Soft Matter, Department of Chemical Engineering and Chemistry, Eindhoven University of Technology, 5600MB Eindhoven, The Netherlands; Laboratory of Macro-Organic Chemistry, Department of Chemical Engineering and Chemistry and Institute for Complex Molecular Systems, Eindhoven University of Technology, 5600MB Eindhoven, The Netherlands*

P. Michel Fransen − *Laboratory of Macro-Organic Chemistry, Department of Chemical Engineering and Chemistry, Eindhoven University of Technology, 5600MB Eindhoven, The Netherlands; SyMO-Chem B.V., 5612 AZ Eindhoven, The Netherlands*

Jose Rodrigo Magana − *Laboratory of Self-Organizing Soft Matter, Department of Chemical Engineering and Chemistry, Eindhoven University of Technology, 5600MB Eindhoven, The Netherlands; Laboratory of Macro-Organic Chemistry, Department of Chemical Engineering and Chemistry and Institute for Complex Molecular Systems, Eindhoven University of Technology, 5600MB Eindhoven, The Netherlands;* orcid.org/0000-0001-8637-1467

Henk M. Janssen − *Laboratory of Macro-Organic Chemistry, Department of Chemical Engineering and Chemistry, Eindhoven University of Technology, 5600MB Eindhoven, The Netherlands; SyMO-Chem B.V., 5612 AZ Eindhoven, The Netherlands;* orcid.org/0000-0002-2588-846X

Complete contact information is available at: https://pubs.acs.org/10.1021/acs.macromol.0c02107

Notes

The authors declare no competing financial interest.

■ ACKNOWLEDGMENTS

The authors thank Remco Tuinier, Álvaro González García, Ronald Tennebroek, Ilse van Casteren, Patrick Stals, Harm Langermans, and Gerard Krooshof for useful suggestions. We acknowledge the Netherlands Organization for Scientific Research (NWO TA grant no. 731.015.205) for financial support.

■ REFERENCES

(1) Król, P. Synthesis Methods, Chemical Structures and Phase Structures of Linear Polyurethanes. Properties and Applications of Linear Polyurethanes in Polyurethane Elastomers, Copolymers and Ionomers. *Prog. Mater. Sci.* **2007**, *52*, 915−1015.

(2) Jaudouin, O.; Robin, J. J.; Lopez-Cuesta, J. M.; Perrin, D.; Imbert, C. Ionomer-Based Polyurethanes: A Comparative Study of Properties and Applications. *Polym. Int.* **2012**, *61*, 495−510.

(3) Borisov, O. V.; Zhulina, E. B.; Leermakers, F. A. M.; Müller, A. H. E. Self-Assembled Structures of Amphiphilic Ionic Block Copolymers: Theory, Self-Consistent Field Modeling and Experiment. *Adv. Polym. Sci.* **2011**, *241*, 57−129.

(4) Birshtein, T. M.; Zhulina, E. B. Scaling Theory of Supermolecular Structures in Block Copolymer-Solvent Systems: 2. Supercrystalline Structures. *Polymer* **1990**, *31*, 1312−1320.

(5) Nagarajan, R.; Ganesh, K. Comparison of Solubilization of Hydrocarbons in (PEO-PPO) Diblock versus (PEO-PPO-PEO) Triblock Copolymer Micelles. *J. Colloid Interface Sci.* **1996**, *184*, 489−499.

(6) Linse, P. Micellization of Polyethylene Oxide)-Poly(Propylene Oxide) Block Copolymers in Aqueous Solution. *Macromolecules* **1993**, *26*, 4437.

(7) Panagiotopoulos, A. Z.; Floriano, M. A.; Kumar, S. K. Micellization and Phase Separation of Diblock and Triblock Model Surfactants. *Langmuir* **2002**, *18*, 2940−2948.

(8) Badi, N.; Lutz, J.-F. Sequence Control in Polymer Synthesis. *Chem. Soc. Rev.* **2009**, *38*, 3383−3390.

(9) Lutz, J. F. Defining the Field of Sequence-Controlled Polymers. *Macromol. Rapid Commun.* **2017**, *38*, 1700582.

(10) Lutz, J.-F.; Ouchi, M.; Liu, D. R.; Sawamoto, M. Sequence-Controlled Polymers. *Science* **2013**, *341*, 1238149.

(11) Perry, S. L.; Sing, C. E. 100th Anniversary of Macromolecular Science Viewpoint: Opportunities in the Physics of Sequence-Defined Polymers. *ACS Macro Lett.* **2020**, *9*, 216−225.

(12) Meier, M. A. R.; Barner-Kowollik, C. A New Class of Materials: Sequence-Defined Macromolecules and Their Emerging Applications. *Adv. Mater.* **2019**, *31*, 1806027.

(13) Gody, G.; Maschmeyer, T.; Zetterlund, P. B.; Perrier, S. Rapid and Quantitative One-Pot Synthesis of Sequence-Controlled Polymers by Radical Polymerization. *Nat. Commun.* **2013**, *4*, 2505.

(14) Ouahabi, A. A.; Kotera, M.; Charles, L.; Lutz, J. F. Synthesis of Monodisperse Sequence-Coded Polymers with Chain Lengths above DP100. *ACS Macro Lett.* **2015**, *4*, 1077−1080.

(15) Sternhagen, G. L.; Gupta, S.; Zhang, Y.; John, V.; Schneider, G. J.; Zhang, D. Solution Self-Assemblies of Sequence-Defined Ionic Peptoid Block Copolymers. *J. Am. Chem. Soc.* **2018**, *140*, 4100−4109.

(16) Chang, L. W.; Lytle, T. K.; Radhakrishna, M.; Madinya, J. J.; Vélez, J.; Sing, C. E.; Perry, S. L. Sequence and Entropy-Based Control of Complex Coacervates. *Nat. Commun.* **2017**, *8*, 1273.

(17) Filippov, S. K.; Verbraeken, B.; Konarev, P. V.; Svergun, D. I.; Angelov, B.; Vishnevetskaya, N. S.; Papadakis, C. M.; Rogers, S.; Radulescu, A.; Courtin, T.; Martins, J. C.; Starovoytova, L.; Hruby, M.; Stepanek, P.; Kravchenko, V. S.; Potemkin, I. I.; Hoogenboom, R. Block and Gradient Copoly(2-Oxazoline) Micelles: Strikingly Different on the Inside. *J. Phys. Chem. Lett.* **2017**, *8*, 3800−3804.

(18) Hoogenboom, R.; Thijs, H. M. L.; Wouters, D.; Hoeppener, S.; Schubert, U. S. Solvent Responsive Micelles Based on Block and Gradient Copoly(2-Oxazoline)S. *Macromolecules* **2008**, *41*, 1581−1583.

(19) Li, F.; Tuinier, R.; van Casteren, I.; Tennebroek, R.; Overbeek, A.; Leermakers, F. A. M. Self-Organization of Polyurethane Pre-Polymers as Studied by Self-Consistent Field Theory. *Macromol. Theory Simul.* **2016**, *25*, 16−27.

(20) Zhulina, E. B.; Borisov, O. V. Theory of Block Polymer Micelles: Recent Advances and Current Challenges. *Macromolecules* **2012**, *45*, 4429−4440.
(21) Lombardo, D.; Kiselev, M. A.; Magazù, S.; Calandra, P. Amphiphiles Self-Assembly: Basic Concepts and Future Perspectives of Supramolecular Approaches. *Adv. Condens. Matter Phys.* **2015**, *2015*, 151683.
(22) Booth, C.; Attwood, D. Effects of Block Architecture and Composition on the Association Properties of Poly(Oxyalkylene) Copolymers in Aqueous Solution. *Macromol. Rapid Commun.* **2000**, *21*, 501−527.
(23) Yan, Y.; Xiong, W.; Li, X.; Lu, T.; Huang, J.; Li, Z.; Fu, H. Molecular Packing Parameter in Bolaamphiphile Solutions: Adjustment of Aggregate Morphology by Modifying the Solution Conditions. *J. Phys. Chem. B* **2007**, *111*, 2225−2230.
(24) Karpe, P.; Ruckenstein, E. The Enzymatic Superactivity in Reverse Micelles: Role of the Dielectric Constant. *J. Colloid Interface Sci.* **1991**, *141*, 534−552.
(25) Wu, H. Correlations between the Rayleigh Ratio and the Wavelength for Toluene and Benzene. *Chem. Phys.* **2010**, *367*, 44−47.
(26) Rasolonjatovo, B.; Gomez, J.-P.; Même, W.; Gonçalves, C.; Huin, C.; Bennevault-Celton, V.; Le Gall, T.; Montier, T.; Lehn, P.; Cheradame, H.; Midoux, P.; Guégan, P. Poly(2-Methyl-2-Oxazoline)-b-Poly(Tetrahydrofuran)-b-Poly(2-Methyl-2-Oxazoline) Amphiphilic Triblock Copolymers: Synthesis, Physicochemical Characterizations, and Hydrosolubilizing Properties. *Biomacromolecules* **2015**, *16*, 748−756.
(27) Che, Y.; Datar, A.; Balakrishnan, K.; Zang, L. Ultralong Nanobelts Self-Assembled from an Asymmetric Perylene Tetracarboxylic Diimide. *J. Am. Chem. Soc.* **2007**, *129*, 7234−7235.
(28) Zhang, L.; Shen, H.; Eisenberg, A. Phase Separation Behavior and Crew-Cut Micelle Formation of Polystyrene-6-Poly(Acrylic Acid) Copolymers in Solutions. *Macromolecules* **1997**, *30*, 1001−1011.

https://dx.doi.org/10.1021/acs.macromol.0c02107
Macromolecules 2021, 54, 2376−2382